Flaming 2π kinks in parametrically driven systems

E. Berrios-Caro,[1] M. G. Clerc,[1] and A. O. Leon[2]
[1]*Departamento de Física, Facultad de Ciencias Físicas y Matemáticas, Universidad de Chile, Casilla 487-3, Santiago, Chile*
[2]*Institute for Materials Research, Tohoku University, Sendai 980-8577, Japan*
(Received 10 July 2016; revised manuscript received 25 October 2016; published 23 November 2016)

Macroscopic extended systems with dissipation and injection of energy can exhibit particlelike solutions. Dissipative kinks with an oscillatory cloak and a family of localized states that connect uniform symmetric states in a magnetic wire forced with a transversal oscillatory magnetic field and in a parametrically driven damped pendula chain are studied. The oscillatory cloak is composed of evanescent waves emitted at the kink position and generated by a resonant mechanism. These waves mediate the kink interaction and generate a family of localized states.

DOI: 10.1103/PhysRevE.94.052217

I. INTRODUCTION

Macroscopic particlelike solutions in extended dissipative systems have been observed in different fields, such as domains in magnetic materials, chiral bubbles in liquid crystals, interfaces in chemical reactions, kinks in granular media, fronts in populations dynamics, liquid crystals, and nonlinear optics, among others [1–3]. Hence, one can infer the universality of particlelike solutions in nonequilibrium systems [4]. Although these states are spatially extended, they exhibit properties typically associated with particles. Consequently, one can characterize them with a family of continuous parameters such as the position and the core width. A natural strategy to obtain these solutions would be to integrate the systems under small variations corresponding to energy dissipation [5]. These types of systems are termed "quasireversible" [6]. Since integrable systems exhibit natural frequencies, a way to force these systems is through temporal modulation of parameters that characterize the system under study. This type of forcing is called parametric [7]. In the past few decades, scientific efforts were focused on improving our understanding of kinks [8]. These solutions are characterized by connecting two equivalent symmetric states. Methods such as variation of parameters and inverse scattering have played a key role in understanding the dynamics of particlelike solutions. However, for dissipative systems—with large injection and dissipation of energy—the dynamic characterization of particlelike solutions remains an open question.

The aim of this article is to study dissipative kinks with an oscillatory cloak and a family of localized states that connect uniform symmetric states. We consider two physical systems that exhibit these structures, namely a magnetic wire forced with a transversal oscillatory magnetic field, and a parametrically driven damped pendula chain. These kink solutions are characterized by the emission of evanescent waves from the front position (cf. Fig. 1). Using an analogy of hopping pattern behavior observable in combustion carried out under controlled conditions [9,10], we consider that propagation of evanescent waves observed in our simulations could be, for want of a more descriptive name, referred to as "*flaming* 2π *kinks*." The oscillatory cloaks are generated by a resonance mechanism between the natural frequency and external forcing. These evanescent waves mediate the kink interaction and generate a family of localized states.

II. FLAMING 2π KINKS IN PARAMETRICALLY DRIVEN MAGNETIC WIRE

The dynamics of ferromagnetic wires are characterized by the normalized magnetization $\mathbf{m}(t,z)$ [11], where $\{z,t\}$ account for the spatial coordinate along the wire and time, respectively. A one-dimensional easy-plane ferromagnetic macroscopic wire is described by the dimensionless Landau-Lifshitz-Gilbert equation [11],

$$\partial_t \mathbf{m} = -\mathbf{m} \times (h\mathbf{e}_x - \beta m_z \mathbf{e}_z + \partial_{zz}\mathbf{m} - \alpha \partial_t \mathbf{m}), \qquad (1)$$

where $\{\mathbf{e}_x,\mathbf{e}_y,\mathbf{e}_z\}$ are the unit vectors along the respective Cartesian axes, $\beta > 0$ accounts for the anisotropy of the wire and it favors configurations where the magnetization lies on the xy plane, the term proportional to α is a Rayleigh-like dissipation function known as Gilbert damping, and it accounts for energy losses, h is the dimensionless intensity of the external magnetic field in the x direction, and the term $\partial_{zz}\mathbf{m}$ corresponds to the Laplacian operator accounting for short-range magnetic interactions [11]. To get an idea of the magnitude of the parameters, for example for $CsNiF_3$, $|\mathbf{m}| \approx 2.2 \times 10^5$ A/m, $\beta \approx 39$, temporal and spatial scales are around 20 ps and 5 nm, and the dissipation parameter is of the order $\alpha \approx 0.02$ [12].

For a positive external field, $h > 0$, the stable equilibrium of the system is the magnetization pointing along the magnetic field, $\mathbf{m} = \mathbf{e}_x$, a magnetization vector aligned with the vertical axis [see Fig. 1(a)]. Perturbations around this equilibrium are characterized by a natural frequency $\omega_0 = \sqrt{h\beta}$ [13]. The dissipation can be counterbalanced by considering a combination of a constant and an oscillatory external magnetic field, $h(t) = H_0 + h_0 \cos(\omega t)$. Notice that the dynamics of the above model (1) conserve the norm of $\mathbf{m}$. Hence, spherical coordinates are an adequate representation to describe the magnetic dynamics of the driven wire. This system has kink solutions. The orientation of magnetization vectors creates a marked spatial pattern: at the left and right ends of the chain, magnetization vectors are predominantly directed along the external field, while at the central part of the chain they undergo a complete rotation, clearly revealing the presence of a kink solution [8]. Figure 1 shows a schematic representation of the magnetic kink solution. Here the spatiotemporal evolution and magnetization components of this particlelike solution were obtained from numerical simulations of Eq. (1). Numerical

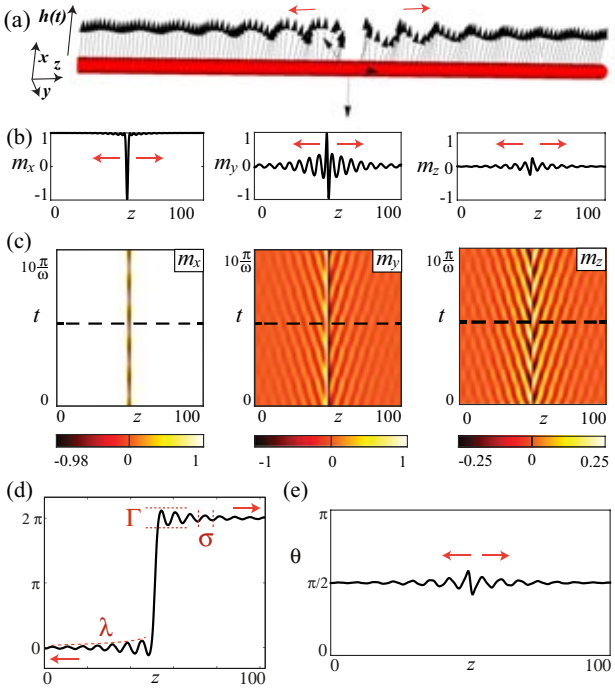

FIG. 1. Flaming 2π kink in a parametrically driven magnetic wire obtained from numerical simulation of Eq. (1) with $h(t) = H_0 + h_0\cos(\omega t)$, $H_0 = 2$, $h_0 = 0.8$, $\omega = 6$, $\beta = 10$, and $\alpha = 0.02$. (a) Schematic representation of magnetization $\mathbf{m}(z)$ upon a driven magnetic wire. (b) Magnetization components of the flaming magnetic kink. (c) Spatiotemporal evolution of the flaming kink. The horizontal dashed line in the diagrams shows the time when the images of (b) were obtained. (d) Corresponding ϕ profile in the spherical representation of the magnetization. $\{\Gamma,\sigma,\lambda\}$ are the amplitude, wavelength, and steepness of the evanescent wave, respectively. (e) Corresponding θ profile in the spherical representation of the magnetization.

simulations were conducted using the fifth-order Runge-Kutta method scheme for temporal integration, finite differences of sixth order for spatial discretization, and Neumann boundary conditions ($\partial_z m = 0$ at the borders). From the spatiotemporal evolution, we can infer that the kink solution is characterized by the emission of evanescent waves from the front position (see Fig. 1). In the quasireversible limit, these waves disappear [5].

To study in detail the flaming kinks, we consider the following spherical representation for magnetization vector $\mathbf{m} = \sin(\theta)[\cos(\phi)\mathbf{e}_x + \sin(\phi)\mathbf{e}_y] + \cos(\theta)\mathbf{e}_z$. In this representation, the magnetization is described by the polar $\theta(t,z)$ and azimuthal $\phi(t,z)$ angles [see Figs. 1(d) and Fig. 1(e)]. When the magnetic anisotropy coefficient is large enough ($\beta \gg 1$), the magnetization vector is located mainly in the xy plane, and the magnetic field acts in the same way as gravity for coupled mechanical oscillators [14,15]. In addition, let us consider small dissipation, an external field, and the scaling relations $|\theta - \pi/2| \sim \alpha \sim h \sim \partial_{zz}\phi \sim 1/\beta \ll 1$ and $\phi \sim \partial_t\phi \sim 1$. Using a spherical representation and this scaling in Eq. (1), one finds at leading order that the polar angle becomes a slave variable $\theta[\phi] \approx \pi/2 + \partial_t\phi/\beta$, and the

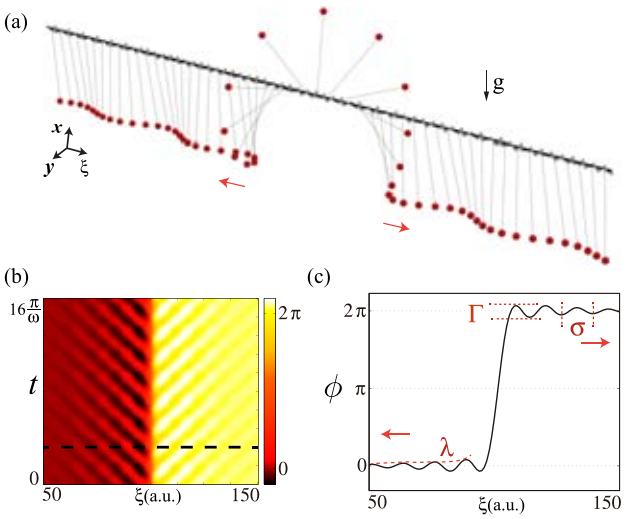

FIG. 2. Flaming 2π kink in a vertically driven chain of coupled pendula obtained from numerical simulation of Eq. (2) with $\omega_0^2(t) = \omega_0^2 + \gamma\cos(\omega t)$, $\omega_0^2 = 1$, $\gamma = 0.3$, $\omega = 1.4$, and $\mu = 0.1$. (a) Schematic representation of a vertically driven dissipative chain of coupled pendula. (b) Spatiotemporal evolution of a motionless flaming kink. (c) Profile of a flaming kink; $\{\Gamma,\sigma,\lambda\}$ are the amplitude, wavelength, and steepness of the evanescent wave, respectively.

azimuthal angle satisfies [14]

$$\partial_{tt}\phi = -\omega_0^2(t)\sin(\phi) + \partial_{\xi\xi}\phi - \mu\partial_t\phi, \tag{2}$$

where $\mu \equiv \alpha\beta$, $\xi \equiv z/\beta^{1/2}$ is a normalized spatial coordinate, and $\omega_0^2(t) = \beta H_0 + \beta h_0\cos(\omega t)$. The aforementioned model stands for a vertically driven dissipative chain of coupled pendula [16]. The parameters $\{\omega_0 \equiv \beta H_0, \gamma \equiv \beta h_0, \mu\}$ account for the natural frequency, the amplitude of the applied force, and the oscillation damping coefficient. Hence, the parametric-driven dissipative sine-Gordon model produces results that considerably resemble the magnetization dynamics in a magnetic chain described with the Landau-Lifshitz-Gilbert equation.

In the next section, we introduce a pendula chain. This set of coupled oscillators is well-described by the sine-Gordon model.

III. FLAMING 2π KINKS IN A PARAMETRICALLY DRIVEN PENDULA CHAIN

Let us consider a plane pendulum of length l_0. The pendulum oscillates in the x-y plane in the presence of gravitation acceleration g pointing along $-\mathbf{e}_x$, as illustrated in Fig. 2. The mechanical motion is governed by $d_{tt}\phi = -\omega_0^2\sin(\phi) - \mu d_t\phi$, where the natural frequency is $\omega_0^2 = g/l_0$, and the damping parameter μ accounts for dissipation. Notice that the above equation is the same as Eq. (2) when the magnetization is uniform, $\partial_{zz}\mathbf{m} = \mathbf{0}$. In the pendulum, as well as in the magnetic system, the angle ϕ accounts for the dynamics in the xy plane. On the other hand, the polar angle of the magnetization vector, $\theta = \arccos(m_z)$, is related to the angular velocity of the pendulum, $\beta(\theta - \pi/2) \approx \partial_t\phi$.

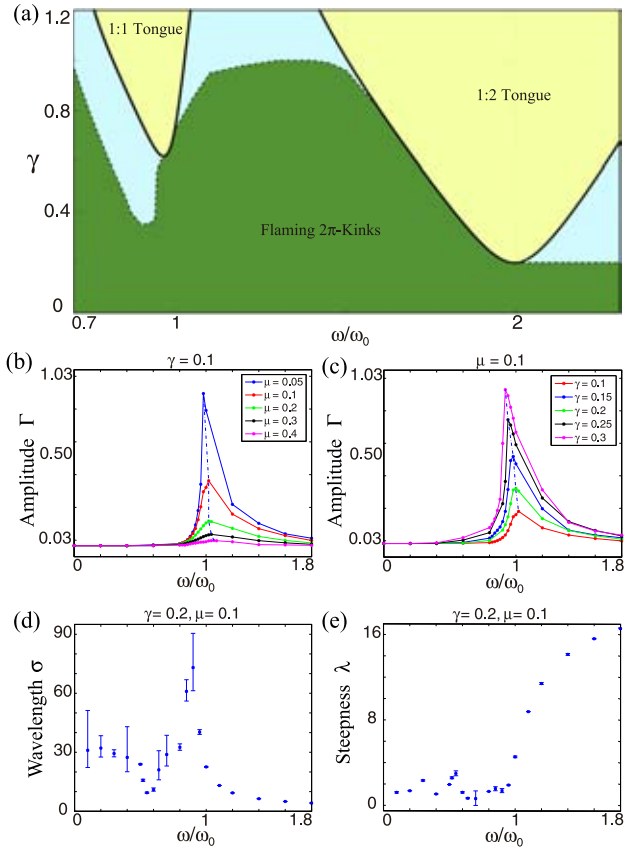

FIG. 3. Characterization of a flaming 2π kink for a vertically driven chain of pendula with $\beta H_0 = 1$. (a) Phase space as a function of frequency and amplitude forcing with $\mu = 0.1$. The tongues account for the strong resonances (1 : 1 and 1 : 2). The flaming 2π kinks are observed in the dark region. (b) Amplitude of evanescent waves Γ as a function of forcing frequency by different dissipation coefficients and forcing intensities (c). Wavelength σ (d) and steepness λ (e) of evanescent waves as a function of frequency forcing ω.

A pendula chain is a system composed of several of the oscillators described above, where each one of them couples to its neighbors by torsion springs, as shown in Fig. 2(a). In the continuum limit, the linear coupling between a pendulum and its neighborhood is written in terms of a Laplacian operator, $\partial_{\xi\xi}\phi$. The torsion spring mechanism is equivalent to the short-range magnetic interaction that couples magnetic moments in ferromagnetic materials. This system in the continuum limit is described by the sine-Gordon model Eq. (2).

Numerical simulations of the sine-Gordon Eq. (2), for small forcing intensities and large dissipation, exhibit 2π kink solutions, that is, the zero equilibrium is connected with the 2π state [8]. Figure 2 shows a schematic representation, a spatiotemporal evolution, and a profile of a flaming 2π kink observed in a vertically driven dissipative chain of coupled pendula. The evanescent waves are well characterized by an amplitude Γ, a steepness λ, and a wavelength σ [see Fig. 2(b)]. Notice there is a good agreement between flaming 2π kinks observed in a forced magnetic wire and a forced chain of pendula. Figure 3(a) illustrates the region of parameter space where the flaming 2π kinks are observed. This region was obtained numerically from Eq. (2) by the persistence of the flaming 2π kink under the small modification of the parameters. From this figure, one can conclude that the flaming 2π kinks are observed in a wide range of frequencies and forcing amplitudes.

To identify the mechanism of flaming 2π kinks, we have computed the amplitude Γ, the wavelength σ, and the spatial damping λ (steepness) [see Figs. 1(d) and 2(c)] of the evanescent waves as a function of the dissipation, frequency, and amplitude of the forcing. The lower panels of Fig. 3 show these results. The amplitude of evanescent waves as a function of the forcing frequency exhibits a resonance when the forcing frequency coincides with the natural frequency ($\omega/\omega_0 \approx 1$). Figure 3 shows this resonance for different dissipation and intensity forcing coefficients. The behavior of these curves is not well described by linear or weakly nonlinear resonance [7,17]. Therefore, one can conclude that the appearance of evanescent waves is the result of a resonance between the parametric forcing and the natural frequency of the pendula. That is, at close to $1:1$ resonance, the amplitude of the evanescent wave is large ($\omega/\omega_0 \approx 1$), which is disclosed in Figs. 3(b) and 3(c). Moreover, in the quasireversal limit ($\{\gamma,\mu\} \ll 1$), the amplitude of the evanescent waves is negligible, and the flaming 2π kinks and 2π kinks are indistinguishable. Likewise, we have characterized the wavelength σ and steepness λ of the evanescent waves as a function of frequency forcing (see the bottom panels of Fig. 3). The steepness increases with frequency higher than the natural frequency. The wavelength exhibits a resonance when the forcing frequency coincides with the natural frequency. This wavelength does not match with the wavelength of the dispersion relation obtained from linear theory around a vertical state. Hence, from the above observations, the properties of evanescent waves are of a nonlinear type.

IV. LOCALIZED FLAMING STATES

Due to the space reflection invariance $\xi \to -\xi$, both kinks connecting 0-2π and 2π-0 exist. The last state is usually termed "antikink." Both states correspond to a front solution connecting two symmetric states. The interaction between spatially monotone fronts in one-dimensional dynamical systems is attractive [18,19], i.e., the fronts attract and eventually annihilate. This scenario changes when fronts exhibit stationary spatial damped oscillations, the front interaction decays at large distance, and it alternates between attractive and repulsive [19]. Therefore, under these conditions, the system under study shows a family of localized structures characterized by having a collapsed snaking bifurcation diagram [19,20]. Namely, in the parameter region that corresponds to the coexistence of localized states, one can clearly see that localized states characterized with a shorter width occur in a wider range of parameters; in contrast, the localized structures of considerable length require precise parameter fine-tuning. In the case of fronts connecting two standing waves (not evanescent), the interaction does not decay quickly with distance, alternating between attractive and repulsive modes. Hence, a family of localized structures with a homoclinic snaking bifurcation diagram is expected [21]. At variance with

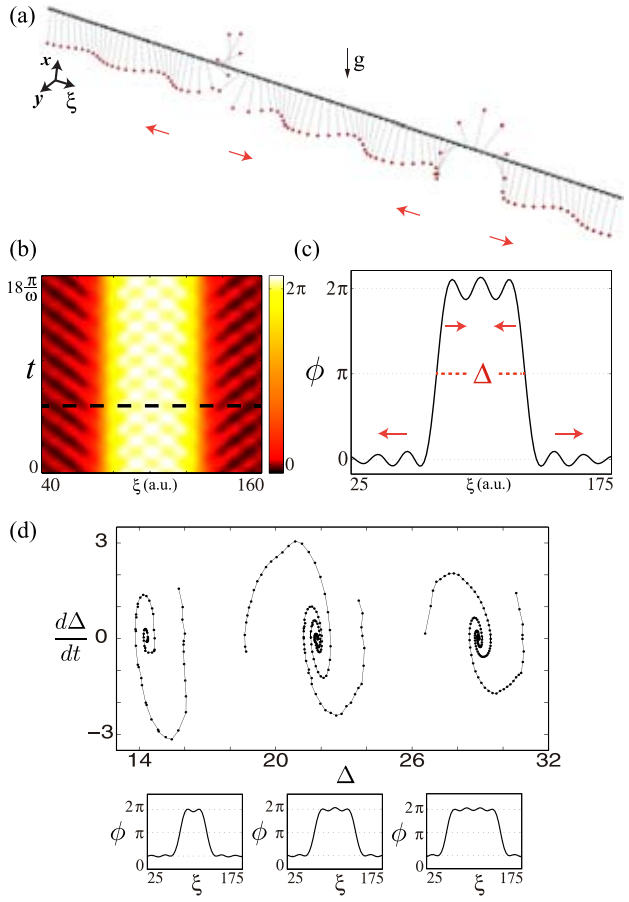

FIG. 4. Localized flaming states in a vertically driven chain of coupled pendula obtained from numerical simulation of Eq. (2) with the same parameters as in Fig. 2. (a) Schematic representation of a bound state composed of a flaming 2π kink and a 2π antikink. Profile at a given time (b) and spatiotemporal temporal evolution (c) of a localized flaming structure. (d) Phase space of the flaming 2π kink position $\{\Delta,\dot{\Delta}\}$ and their stationary localized flaming states, respectively.

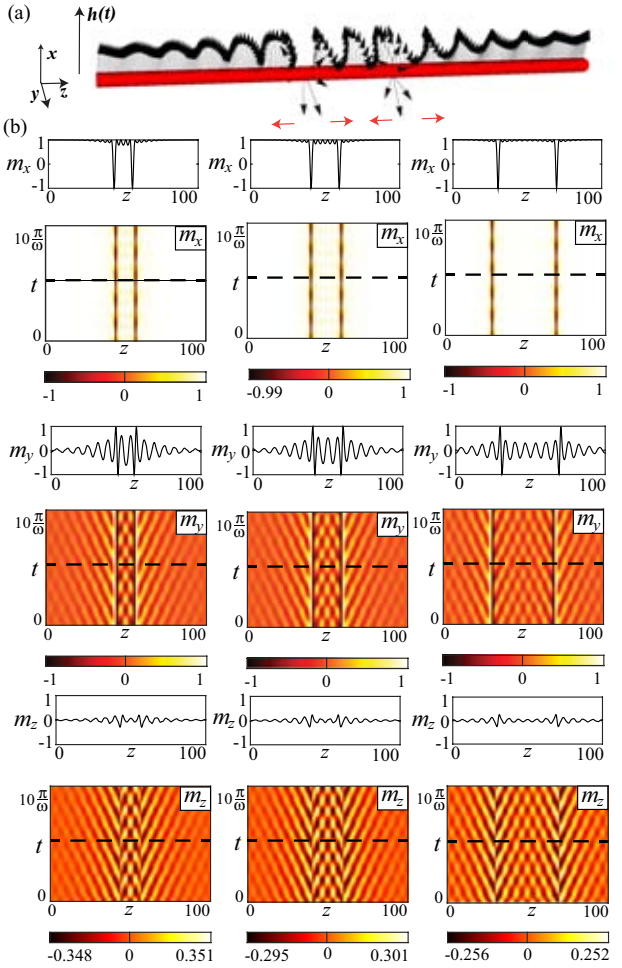

FIG. 5. Flaming localized states in a magnetic wire forced with a transversal oscillatory magnetic field. (a) Arrow representation of a bound state composed of a flaming 2π kink and a flaming 2π antikink at a given time. (b) Cartesian components of the magnetization for three particlelike states with different widths. For every magnetization component, the magnetization profile is shown above the corresponding spatiotemporal diagram. The horizontal line in the diagram shows the instant when the profiles were obtained. For this figure, we used the same parameters as in Fig. 1.

the previous description, localized structures obtained from kink interaction coexist simultaneously.

In our case of flaming 2π kinks, the interaction is governed by evanescent waves. Figure 4 shows a localized structured composed of a flaming 2π kink and a flaming 2π antikink observed in a vertically driven chain of coupled pendula. Monitoring periodically the flaming 2π kink with forcing frequency ω (extended Poincaré section), the flaming 2π kinks are motionless. Indeed, in the extended Poincaré section, the flaming 2π kinks are stationary and characterized with spatial damping oscillations [similar to that shown in Fig. 2(b)], that is, in the extended Poincaré section $\phi(x \to \pm\infty) \to \phi_0 e^{\mp\lambda x}\sin(\frac{2\pi x}{\sigma})$. Hence, it is natural to expect that the interaction between the kinks will be dominated by contributions from the oscillation tails. To prove this, let us consider a pair of a kink and an antikink, located a considerable distance from each other. Let Δ be the distance between the positions of each kink [see Fig. 4(b)]. Using the general theory of kink interaction [19] and assuming a temporal scale separation, for systems with inertia upon the extended Poincaré section, the dynamics between the kink could be described by

$$\ddot{\Delta} + \mu\dot{\Delta} = -a\Gamma e^{\mp\lambda\Delta}\sin\left(\frac{2\pi\Delta}{\sigma} + \varphi_o\right), \qquad (3)$$

where the phenomenological coefficients $\{a,\varphi_o,\Gamma\}$ are numerically computed. The dynamics of the kink interaction satisfies a Newton-type equation with a force that decays exponentially with distance and alternates between positive and negative values. Hence, the system has a family of steady states of the form $\Delta_n = (\pi n - \varphi_o)/\sigma$ for large enough $n = \{1,2,\dots\}$, which alternate between node and saddle

equilibria. Figure 4(d) illustrates in its lower panels three stable localized structures with different sizes. To confirm the dynamics predicted by the previous phenomenological model, Eq. (3), we have reconstructed the phase space for the flaming kink interaction by numerically measuring the evolution of the position $\Delta(t)$ and the rate of change $\dot{\Delta}(t)$ of a pair of kinks. Figure 4(d) shows the phase space of the flaming 2π kink position and its stationary localized flaming states, respectively. This phase space presents a quite good agreement with the phenomenological model Eq. (3). Then the results extracted from the extended Poincaré section are consistent.

We can infer that the interaction between flaming kinks is mediated by the evanescent waves, which permits the generation of bound states (cf. Fig. 4). To verify the robustness of this property, we have conducted numerical simulations of magnetic wire forced with a transversal oscillatory magnetic field. Figure 5 shows three of the flaming localized states obtained for the same parameters used in Fig. 1. Those figures were obtained using the following type of initial condition: $\mathbf{m} = \cos[\phi_k(z - z_k) + \phi_{ak}(z - z_{ak})]\mathbf{e}_x + \sin[\phi_k(z - z_k) + \phi_{ak}(z - z_{ak})]\mathbf{e}_y$, where $\{\phi_k(z - z_{ak}), \phi_{ak}(z - z_{ak})\}$ are, respectively, the flaming 2π kink and the flaming 2π antikink solution of sine-Gordon, and the coordinates $\{z_k, z_{ak}\}$ stand for the positions of the flaming kinks. These numerical simulations show that the family of localized states formed by the flaming kinks are a common phenomenon of parametric systems that exhibit kinks. Note that for small bound states there is a standing wave connecting the kink positions [see Fig. 5(c)]. However, as the width of the flaming localized states becomes larger, a standing wave is observed in the center only, while propagative waves are observed near kink positions. This structure is a direct consequence of the evanescent nature of the waves emitted by the flaming kinks.

V. CONCLUSIONS AND REMARKS

We have studied dissipative kinks with an oscillatory cloak and a family of flaming localized states that connect uniform symmetrical states in a magnetic wire forced with a transversal oscillatory magnetic field and in a parametrically driven damped pendula chain. We have termed these particlelike solutions "flaming kinks." The oscillatory cloak is composed of evanescent waves from the kink position and is generated by a resonant mechanism between the frequency of parametric forcing and the natural frequency of the extended oscillator. These evanescent waves mediate the kink interaction and generate a family of localized states. Using an extended Poincaré section and numerical simulations, we have inferred the flaming kink interaction. Numerical simulations of a magnetic wire forced with a transversal oscillatory magnetic field and a parametrically driven damped pendula chain show quite fair agreement with our findings.

We have characterized the parameter space for a parametrically driven damped pendula chain where the flaming 2π kinks are observed. However, elucidating the mechanisms by which these flaming 2π kinks disappear is in progress. Localized particles in two dimensions with evanescent waves have been observed in droplets on a vertically driven fluid [22]. The dynamics of these two-dimensional particles is similar to those seen in the flaming kinks. Study in this direction is in progress.

ACKNOWLEDGMENTS

We acknowledge the referee for valuable suggestions. M.G.C. gratefully acknowledges the financial support of FONDECYT projects 1150507. E.B.-C. gratefully acknowledges the financial support of CONICYT through Becas Magister Nacional 2015, Contract No. 22151824. A.O.L. gratefully acknowledges the JSPS KAKENHI Grant No. 26103006.

[1] L. M. Pismen, *Patterns and Interfaces in Dissipative Dynamics* (Springer, Berlin, 2006).

[2] M. Cross and H. Greenside, *Pattern Formation and Dynamics in Nonequilibrium Systems* (Cambridge University Press, New York, 2009).

[3] *Localized States in Physics: Solitons and Patterns*, edited by O. Descalzi, M. G. Clerc, R. Residori, and G. Assanto (Springer Science & Business Media, Berlin, 2011).

[4] G. Nicolis and I. Prigogine, *Self-organization in Nonequilibrium Systems* (Wiley, New York, 1977).

[5] Y. S. Kivshar and B. A. Malomed, Dynamics of solitons in nearly integrable systems, Rev. Mod. Phys. **61**, 763 (1989).

[6] M. Clerc, P. Coullet, and E. Tirapegui, Lorenz bifurcation: Instabilities in quasireversible systems, Phys. Rev. Lett. **83**, 3820 (1999); The stationary instability in quasi-reversible systems and the Lorenz pendulum, Int. J. Bifurcation Chaos **11**, 591 (2001).

[7] L. D. Landau and E. M. Lifshiftz, *Mechanics*, Course of Theoretical Physics Vol. 1 (Pergamon, Oxford, 1976).

[8] O. M. Braun and Y. Kivshar, *The Frenkel-Kontorova Model: Concepts, Methods, and Applications* (Springer Science & Business Media, Berlin, 2013).

[9] J. D. Kelley, G. H. Gunaratne, A. Palacios, and J. Shulman, Modal decomposition and normal form for hydrodynamic flows: Examples from cellular flame patterns, Eur. Phys. J. Spec. Top. **204**, 119 (2012).

[10] P. Blomgren, S. Gasner, and A. Palacios, Hopping behavior in the Kuramoto-Sivashinsky equation, Chaos **15**, 013706 (2005).

[11] I. D. Mayergoyz, G. Bertotti, and C. Serpico, *Nonlinear Magnetization Dynamics in Nanosystems* (Elsevier, Oxford, 2009).

[12] D. Urzagasti, D. Laroze, M. G. Clerc, and H. Pleiner, Breather soliton solutions in a parametrically driven magnetic wire, Europhys. Lett. **104**, 40001 (2013).

[13] M. G. Clerc, S. Coulibaly, and D. Laroze, Localized states and non-variational Ising-Bloch transition of a parametrically driven easy-plane ferromagnetic wire, Physica D **239**, 72 (2010).

[14] H. J. Mikeska, Solitons in a one-dimensional magnet with an easy plane, J. Phys. C **11**, L29 (1978).

[15] K. M. Leung, Mechanical properties of double-sine-Gordon solitons and the application to anisotropic Heisenberg ferromagnetic chains, Phys. Rev. B **27**, 2877 (1983).

[16] M. G. Clerc, S. Coulibaly, and D. Laroze, Parametrically driven instabilities in quasi-reversal systems, Int. J. Bifurcation Chaos **19**, 3525 (2009).

[17] N. N Bogoliubov and Y. A. Mitropolski, *Asymptotic Methods in the Theory of Non-Linear Oscillations* (Gordon and Breach, New York, 1961).

[18] K. Kawasaki and T. Otha, Kink dynamics in one-dimensional nonlinear systems, Physica (Amsterdam) **116A**, 573 (1982).

[19] P. Coullet, Localized patterns and fronts in nonequilibrium systems, Int. J. Bifurcation Chaos **12**, 2445 (2002).

[20] P. Coullet, L. Gil, and D. Repaux, Defects and Subcritical Bifurcations, Phys. Rev. Lett. **62**, 2957 (1989).

[21] M. G. Clerc, C. Fernández-Oto, and S. Coulibaly, Pinning-depinning transition of fronts between standing waves, Phys. Rev. E **87**, 012901 (2013).

[22] S. Protiere, A. Boudaoud, and Y. Couder, Particle-wave association on a fluid interface, J. Fluid Mech. **554**, 85 (2006).